Stem Cell Research 47 (2020) 101892

Contents lists available at ScienceDirect

Stem Cell Research

journal homepage: www.elsevier.com/locate/scr

Lab resource: Stem Cell Line

Generation of human induced pluripotent stem cell line from Alzheimer's disease patient with PSEN2 N141I mutation using integration-free non-viral method

Harry Murti[a,e,1], Kelvin Pieknell[b,d,1], Indra Bachtiar[a,e], Yanuar Alan Sulistio[b,c,*], Sang-Hun Lee[b,c,d]

[a] Department of Translational Research Stem Cell, Stem Cell and Cancer Institute, PT. Kalbe Farma Tbk., Jakarta, Indonesia
[b] Hanyang Biomedical Research Institute, Hanyang University, Seoul, Republic of Korea
[c] Department of Biochemistry and Molecular Biology, College of Medicine, Hanyang University, Seoul, Republic of Korea
[d] Graduate School of Biomedical Science and Engineering, Hanyang University, Seoul, Republic of Korea
[e] ReGeniC Laboratory, PT. Bifarma Adiluhung, Jakarta, Indonesia

A B S T R A C T

Induced pluripotent stem cell (iPSC) line HUi001-A was reprogrammed from skin fibroblasts via non-integrating, virus free self-replicating RNA. Skin fibroblasts from an 81-year-old female Caucasian familial Alzheimer's disease patient of Volga German family carrying N141I mutation in the PSEN2 gene (familial AD4, clinical summary confirmed Alzheimer's disease) was obtained from the Coriell Institute (AG09908). Generated iPSCs were characterized and pluripotency was confirmed.

Resource Table

Unique stem cell line identifier	HUi001-A
Alternative name(s) of stem cell line	iPSC AG09908R
Institution	Hanyang Biomedical Research Institute, Hanyang University, Seoul, Korea
Contact information of distributor	Yanuar Alan Sulistio, Ph.D
Type of cell line	iPSC
Origin	Human
Additional origin info	Age: 81Sex: FemaleEthnicity: German
Cell Source	Skin Fibroblast
Clonality	Single Clone
Method of reprogramming	Transgene free, non-integrating & self-replicating RNA
Genetic Modification	No
Type of Modification	No
Associated disease	Alzheimer's disease, familial, type 4 Presenilin 2
Gene/locus	PSEN2 / locus: 1q42.13
Method of modification	N/A
Name of transgene or resistance	N/A
Inducible/constitutive system	N/A
Date archived/stock date	02/02/2020
Cell line repository/bank	N/A
Ethical approval	The Coriell Institute for Medical Research (Camden, NJ), provider of the fibroblast line (AG09908), guarantees that the skin sample was collected under IRB approval and patient informed consent.

1. Resource utility

PSEN2 (N141I) is a rare mutation for inducing familial Alzheimer's Disease but it has a very high penetrance. The iPSC line generated in this study iPSC line can be utilised for in vitro modelling to study Alzheimer's Disease pathophysiology and PSEN2 biology.

2. Resource details

Skin fibroblasts from an 81-year-old female Alzheimer's disease patient of Volga German family were obtained from the Coriell Institute (AG09908) (Rogaev et al., 1995). This fibroblast carries early-onset familial Alzheimer's Disease-linked Presenilin-2 (PSEN2) single point mutation (N141I) which increase the production of pathogenic $A\beta_{42}$ species (Walker et al., 2005). Moreover, accumulating data suggested that PSEN2 (N141I) mutation may also negatively affects cellular energetics through Ca^{2+}-mediated mitochondrial destabilization (Rossi

* Corresponding author at: Hanyang Biomedical Research Institute, Hanyang University, Seoul, Republic of Korea.
E-mail address: sulistio@hanyang.ac.kr (Y.A. Sulistio).
[1] These authors contributed equally to this work.

https://doi.org/10.1016/j.scr.2020.101892
Received 9 April 2020; Received in revised form 4 May 2020; Accepted 21 June 2020
Available online 29 June 2020

Table 1
Characterization and validation.

Classification	Test	Result	Data
Morphology	Photography	Normal (human ESC-like morphology). Scale bar, 200 μm.	Fig. 1C
Phenotype	Immunocytochemistry	Expression of pluripotency markers OCT4, LIN28, NANOG, TRA-1-60, TRA-1-81, SSEA-3, SSEA-4, SOX2. Scale Bar, 200 μm.	Fig. 1C
	Alkaline Phosphatase (AP) activity	AP-positive colonies	Fig. 1C
	RT-qPCR	Cells expressed *POU5F1* (OCT4), *NANOG*, *SOX2*, *LIN28A*, *ZFP42* (REX1), *CDH1* (E-CAD)	Fig. 1D
Genotype	Karyotype (G-banding)	46, XX, t(13;20)(q12;p11.2), resolution: 550 bands	Fig. 1B
Identity	Microsatellite PCR (mPCR) OR	N/A	N/A
	STR analysis	100% match in 16 tested sites	Submitted in archive with journal
Mutation analysis	Sequencing	Heterozygous substitution (A > T at 787) in the PSEN2 gene resulting to N141I missense mutation	Fig. 1A
	Southern Blot OR WGS	N/A	N/A
Microbiology and virology	Mycoplasma	Mycoplasma testing by RT-PCR was Negative	Supplementary Fig. 1
Differentiation potential	PluriTest	Pluripotency score: 20.11 Novelty score: 1.59. Pluripotency and novelty score confirm pluripotent state.	Fig. 1G
	Directed differentiation (Immunocytochemistry)	FOXA2 (endoderm), BRACHYURY (mesoderm), and TUJ-1 (ectoderm) positive cell. Scale Bar, 100 μm.	Fig. 1H
	Directed differentiation (RT-qPCR)	*GATA4* (endoderm), *TBXT* (mesoderm) & *PAX6* (ectoderm).	Fig. 1I

et al., 2020).

We generated patient-derived iPSC line (HUi001-A) using self-replicating RNA reprogramming vector, ReproRNA™-OKSGM Kit (STEMCELL Technologies) which was followed by isolation and expansion as individual clone (Table 1). Heterozygous substitute (A > T at nucleotide 787) in the PSEN2 gene resulting to N141I missense mutation was confirmed and was consistent with the parental fibroblast lines (Fig. 1A). Selected clone for iPSC line showed chromosome 13 to chromosome 20 translocation with cytogenetic finding of 46, XX, t(13;20)(q12;p11.2) (Fig. 1B). Of note, the parental fibroblast line has been reported to have unstable karyotype and this chromosomal abnormality is not associated with any known disorder. The generated iPSC line was authenticated against its initial fibroblast lines using short tandem repeat (STR) profiling. The iPSC line showed typical human PSCs morphology, with distinct edges and a high nucleus-to-cytoplasm ratio (Fig. 1C). It also showed positive staining for pluripotent markers OCT4, LIN28, NANOG, TRA-1-60, TRA-1-81, SSEA-3, SSEA-4, and alkaline phosphatase (Fig. 1C). Furthermore, the iPSC has high level of *POU5F1* (OCT4), *NANOG*, *SOX2*, *LIN28A*, *ZFP42* (REX1), *CDH1* (E-CAD) mRNA expression which are comparable to H9 hESC (Fig. 1D), while fibroblast marker gene *S100A4* (FSP1) expression was lost after successful reprogramming (Fig. 1E). Self-replicating RNA reprogramming vector (puromycin resistance gene) expression was absent when compared to positive control (reprogramming vector-transfected fibroblast, 10-day post transfection) to the level comparable to untransfected donor fibroblast (Fig. 1F). Pluripotency was further confirmed using PluriTest (Müller et al., 2011), with the HUi001-A line obtained high pluripotency (20.11) and low novelty score (1.59) which indicates a pluripotent stem cell identity (Fig. 1G). In vitro trilineage differentiation potential of HUi001-A was confirmed by directed differentiation into endoderm, mesoderm, and ectoderm, as indicated by FOXA2, BRACHYURY (T), and TUJ1 immunofluorescence staining (Fig. 1H) and *GATA4, TBXT*, *PAX6* qPCR (Fig. 1I), respectively. The generated HUi001-A iPSC did not contain mycoplasma contamination (Fig. S1).

3. Materials and methods

3.1. Reprogramming of skin fibroblasts into iPSCs

Fibroblasts were plated on Matrigel-coated dish and cultured in DMEM/F12 (Gibco, #11330-032) with 10% FBS (Gibco, #26140-079), 1X Glutamax (Gibco, #35050-061), and Recombinant B18R Protein (STEMCELL Technologies, #78075) before reprogramming which was carried out using the ReproRNA™-OKSGM Kit (STEMCELL Technologies, #05930) according to the manufacturer's protocol. iPSC colonies were manually transferred to another Matrigel-coated dish for isolation and expansion and maintained in mTeSR™ (STEMCELL Technologies, #85850) at 37 °C and 5% CO_2.

3.2. DNA sequencing

Sanger DNA sequencing of the iPSCs was conducted by Macrogen on PSEN2 gene (Seoul, Korea).

3.3. Karyotyping

Karyotyping of the iPSCs was performed by GenDix (Seoul, Korea) at 550 band resolution.

3.4. Immunofluorescence staining

iPSC cultured cells were fixed with 4% paraformaldehyde (PFA) in PBS and blocked in 0.3% Triton X-100 with 1% BSA for 1 h, then incubated with primary antibodies (Table 2) overnight at 4 °C following by secondary antibody for 1 h at RT. The stained cells were mounted with VECTASHIELD antifade mounting medium with DAPI (Vector Laboratories, #H-1200), and photographs were obtained by an epifluorescence microscope (Leica).

3.5. Alkaline phosphatase staining

iPSC cultured cells were fixed with 4% paraformaldehyde (PFA) in PBS, then stained with alkaline phosphatase staining solution (Sigma, #10713023001) and photographed with a camera that was attached to a light microscope (Olympus).

3.6. Quantitative RT-PCR analysis

Total RNA was prepared using the TRIzol™ Reagent (Invitrogen, #15596026) through the RNA isolation protocol. cDNA synthesis was carried out using a SuperScript™ kit (Invitrogen, #18080044). Quantitative RT-PCR was performed on a CFX96TM Real-Time System using iQ™ SYBR® Green Supermix (Bio-Rad, #1708882) and gene expression levels were determined relative to GAPDH levels. Primer information is shown in Table 2.

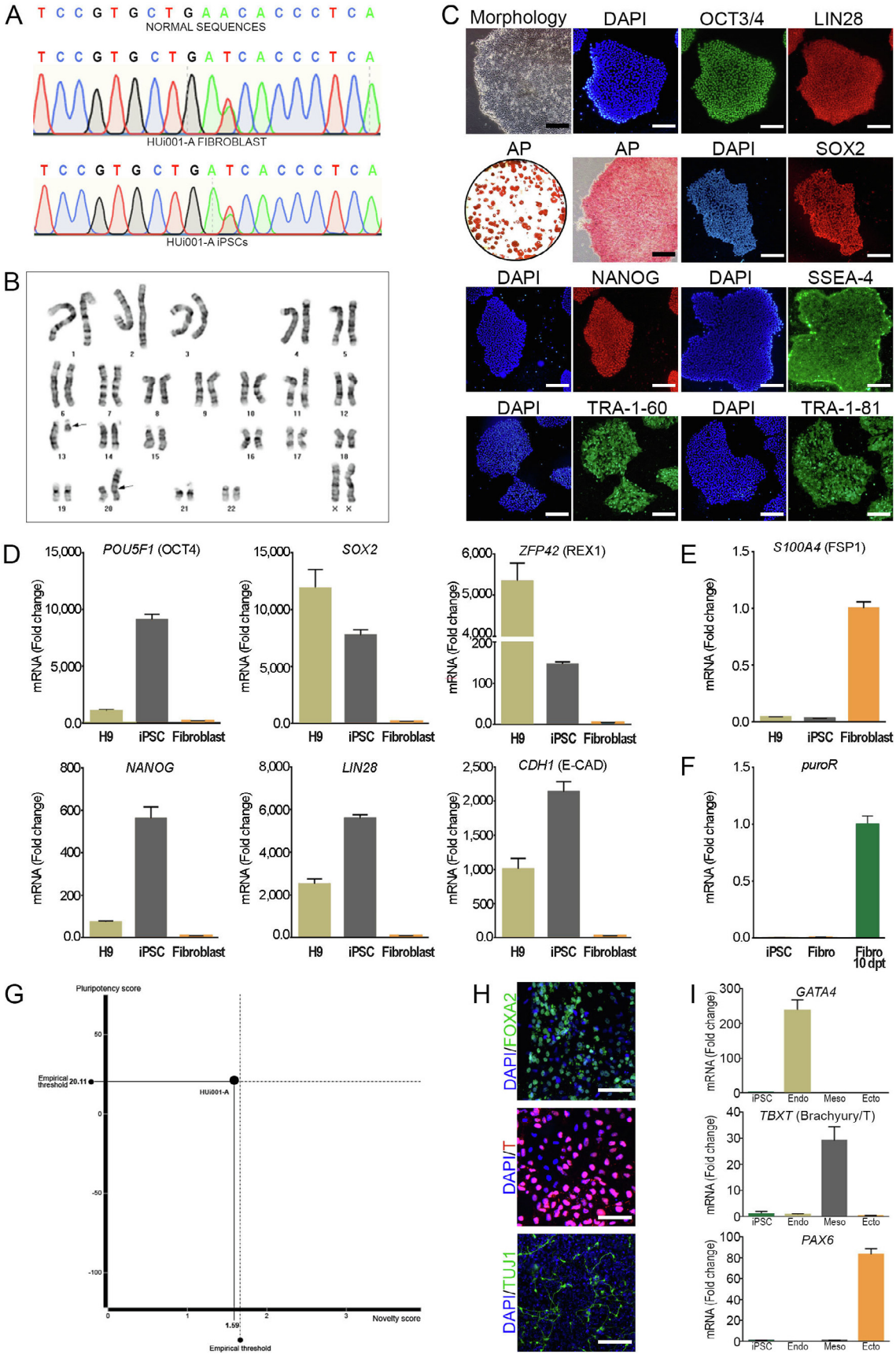
A
T C C G T G C T G A A C A C C C T C A
NORMAL SEQUENCES
T C C G T G C T G A T C A C C C T C A
HUi001-A FIBROBLAST
T C C G T G C T G A T C A C C C T C A
HUi001-A iPSCs
B
C
Morphology
DAPI
OCT3/4
LIN28
AP
AP
DAPI
SOX2
DAPI
NANOG
DAPI
SSEA-4
DAPI
TRA-1-60
DAPI
TRA-1-81
D
POU5F1 (OCT4)
SOX2
ZFP42 (REX1)
NANOG
LIN28
CDH1 (E-CAD)
mRNA (Fold change)
H9
iPSC
Fibroblast
E
S100A4 (FSP1)
F
puroR
iPSC
Fibro
Fibro 10 dpt
G
Pluripotency score
Empirical threshold 20.11
HUi001-A
Novelty score
1.59
Empirical threshold
H
DAPI/FOXA2
DAPI/T
DAPI/TUJ1
I
GATA4
TBXT (Brachyury/T)
PAX6
iPSC
Endo
Meso
Ecto

Fig. 1.

Table 2
Reagents details.

Antibodies used for immunocytochemistry			
	Antibody	Dilution	Company Cat # and RRID
Pluripotency Markers	Mouse anti-OCT4	1:200	BD Biosciences Cat# 561555, RRID:AB_10715577
Pluripotency Markers	Mouse anti-TRA-1-60	1:200	STEMCELL Technologies Cat# 60064, RRID:AB_2686905
Pluripotency Markers	Mouse anti-TRA-1-81	1:200	STEMCELL Technologies Cat# 60065, RRID:AB_2721032)
Pluripotency Markers	Rat anti-SSEA3	1:200	STEMCELL Technologies Cat# 60061 RRID:AB_1118554
Pluripotency Markers	Mouse anti-SSEA4	1:200	STEMCELL Technologies Cat# 60062, RRID:AB_2721031
Pluripotency Markers	Rabbit anti-LIN28A	1:500	Proteintech Cat# 11724-1-AP, RRID:AB_2135039
Pluripotency Markers	Rabbit anti-SOX2	1:200	Millipore Cat# AB5603, RRID:AB_2286686
Pluripotency Markers	Rabbit anti-NANOG	1:200	Cell Signaling Technology Cat# 4903, RRID:AB_10559205
Differentiation Markers (Endoderm)	Mouse anti-FOXA2	1:200	Santa Cruz Biotechnology Cat# sc-374376, RRID:AB_10989742
Differentiation Markers (Mesoderm)	Rabbit anti-BRACHYURY	1:200	Abcam Cat# ab20680, RRID:AB_727024
Differentiation Markers (Ectoderm)	Rabbit anti-TUBULIN-β-3	1:200	BioLegend Cat# 802001, RRID:AB_2564645
Secondary antibodies	Goat anti-mouse Alexa Fluor 488	1:500	Thermo Fisher Scientific Cat# A28175, RRID:AB_2536161
Secondary antibodies	Goat anti-rabbit Cy™3	1:500	Jackson ImmunoResearch Labs Cat# 111-165-144, RRID:AB_2338006
Secondary antibodies	Donkey anti-rat Cy™3	1:500	Jackson ImmunoResearch Labs Cat# 712-165-153, RRID:AB_2340667

Primers		
	Target	Forward/Reverse primer (5′-3′)
Mutation Analysis (Sequencing)	*PSEN2*	CTA GCA GGT CCA GAA TCA CT
Pluripotency Markers (qPCR)	*POUF51* (OCT4)	Forward: GGG AGA TTG ATA ACT GGT GTG TT Reverse: GTG TAT ATC CCA GGG TGA TCC TC
Pluripotency Markers (qPCR)	*NANOG*	Forward: TGC CTC ACA CGG AGA CTG Reverse: GCT ATT CTT CGG CCA GTT
Pluripotency Markers (qPCR)	*SOX2*	Forward: CAA AAA TGG CCA TGC AGG TT Reverse: AGT TGG GAT CGA ACA AAA GCT ATT
Pluripotency Markers (qPCR)	*LIN28A*	Forward: CGG GCA TCT GTA AGT GGT TC Reverse: CAG ACC CTT GGC TGA CTT CT
Pluripotency Markers (qPCR)	*ZFP42* (REX1)	Forward: CCT GCA GGC GGA AAT AGA AC Reverse: GCA CAC ATA GCC ATC ACA TAA GG
Pluripotency Markers (qPCR)	*CDH1* (E-CAD)	Forward: TGG TTC AAG CTG CTG ACC TTC Reverse: ACG ACG TTA GCC TCG TTC T
Residual self-replicating RNA reprogramming vector (qPCR)	*Puromycin Resistance Gene* (*puroR*)	Forward: GCA ACC TCC CCT TCT ACG AGC Reverse: TCA GGC ACC GGG CTT
Fibroblast specific marker gene (qPCR)	*S100A4* (FSP1)	Forward: TCT TGG TTT GAT CCT GAC TGC T Reverse: GCC CGA GTA CTT GTG GAA GG
Differentiation Markers (Endoderm)	*GATA4*	Forward: CTG GCC TGT CAT CTC ACT ACG Reverse: GGT CCG TGC AGG AAT TTG AGG
Differentiation Markers (Mesoderm)	*TBXT* (Brachyury/T)	Forward: TAA GGT GGA TCT TCA GGT AGC Reverse: CAT CTC ATT GGT GAG CTC CCT
Differentiation Markers (Ectoderm)	*PAX6*	Forward: AAC AGA CAC AGC CCT CAC AAA CA Reverse: CGG GAA CTT GAA CTG GAA CTG AC
House-Keeping Genes (qPCR)	*GADPH*	Forward: TTG AGG TCA ATG AAG GGG TC Reverse: GAG GTG AAG GTC GGA GTC A

3.7. PluriTest analysis

Total RNA was extracted using TRIzol™ Reagent. Strand library was constructed using TruSeq Stranded mRNA LT using high quality RNA (RIN = 10) as input. RNA Sequencing was done by Macrogen (Seoul, Korea) using Illumina NovaSeq 6000 system. The resulting raw data files were uploaded to PluriTest server (www.pluritest.org), and the resulting pluripotency and novelty score are reported (Müller et al., 2011).

3.8. In vitro trilineage differentiation

Directed differentiation of iPSC colonies to the three germ layers was carried out. Endoderm differentiation was induced by basal differentiation media containing 20 ng/mL Activin A (Peprotech, #120-14E), and 3 μM CHIR (Stemgent, #04-0004) for 7 days. Mesoderm was induced using basal differentiation media containing 2 ng/mL Activin A (Peprotech, #120-14E) and 40 ng/mL BMP4 (Peprotech, #120-05) for 7 days. Ectoderm differentiation was induced by basal differentiation media containing 10 μM SB-431542 (TOCRIS, #1614) and 100 ng/mL Noggin (Peprotech, #120-10C) for 12 days. For basal differentiation media, 1X N2 supplement (Gibco, #17502-048), 1X B27 without retinoic acid (Gibco, #12587-010), 1X Glutamax (Gibco, #35050-061), and 200 μM Ascorbic acid were supplemented into DMEM/F12 (Gibco, #11330-032).

3.9. STR analysis

STR analysis of 16 sites was performed by Macrogen (Seoul, Korea) using AmpFISTR®Identifiler® PCR Amplification KIT.

3.10. Mycoplasma test

Mycoplasma contamination was conducted using e-Myco™ Mycoplasma PCR detection kit (iNtRON Biotechnology) according to the manufacturer's protocol.

Declaration of Competing Interest

The authors declare the following financial interests/personal relationships which may be considered as potential competing interests: H.M. and I. B. are employee of Kalbe Group (Indonesia). This study is

partly funded by Stem Cell and Cancer Institute Kalbe.

Acknowledgement

This work was supported by 2017R1A5A2015395 (MRC grant), 2020M3A9D8039925, 2017M3A9B4062415, funded by the National Research Foundation of Korea (NRF) of the Ministry of Science and ICT, Republic of Korea and PT Kalbe Farma, Tbk, Indonesia.

Appendix A. Supplementary data

Supplementary data to this article can be found online at https://doi.org/10.1016/j.scr.2020.101892.

References

Müller, F.-J., Schuldt, B.M., Williams, R., Mason, D., Altun, G., Papapetrou, E., Danner, S., Goldman, J.E., Herbst, A., Schmidt, N.O., Aldenhoff, J.B., Laurent, L.C., Loring, J.F., 2011. A bioinformatic assay for pluripotency in human cells. Nat. Methods 8, 315–317. https://doi.org/10.1038/nmeth.1580.

Rogaev, E.I., Sherrington, R., Rogaeva, E.A., Levesque, G., Ikeda, M., Liang, Y., Chi, H., Lin, C., Holman, K., Tsuda, T., Mar, L., 1995. Familial Alzheimer's disease in kindreds with missense mutations in a gene on chromosome 1 related to the Alzheimer's disease type 3 gene. Nature 376 (6543), 775–778. https://doi.org/10.1038/376775a0.

Rossi, A., Rigotto, G., Valente, G., Giorgio, V., Basso, E., Filadi, R., Pizzo, P., 2020. Defective mitochondrial pyruvate flux affects cell bioenergetics in Alzheimer's disease-related models. Cell Reports 30, 2332–2348. https://doi.org/10.1016/j.celrep.2020.01.060.

Walker, E.S., Martinez, M., Brunkan, A.L., Goate, A., 2005. Presenilin 2 familial Alzheimer's disease mutations result in partial loss of function and dramatic changes in Aβ 42/40 ratios. J. Neurochem. 92 (2), 294–301.